

## Phase Relations of the $\text{Cu}_2\text{S-Bi}_2\text{S}_3$ System

Asahiko SUGAKI\* and Hiromi SHIMA\*

(Received December 7, 1972)

### Introduction

As the copper-bismuth sulfide minerals, wittichenite ( $3\text{Cu}_2\text{S}\cdot\text{Bi}_2\text{S}_3$ ), klaprothite ( $3\text{Cu}_2\text{S}\cdot 2\text{Bi}_2\text{S}_3$ ), emplectite ( $\text{Cu}_2\text{S}\cdot\text{Bi}_2\text{S}_3$ ), cuprobismutite ( $\text{Cu}_2\text{S}\cdot\text{Bi}_2\text{S}_3$  or  $3\text{Cu}_2\text{S}\cdot 4\text{Bi}_2\text{S}_3$ ), and dognacskite ( $\text{Cu}_2\text{S}\cdot 2\text{Bi}_2\text{S}_3$ ) have been reported until now in natural occurrence, but the validity of their existence except wittichenite and emplectite has been questioned and discussed many times by numerous workers.

In 1868, Petersen<sup>1)</sup> and Sandberger<sup>2)</sup> gave a chemical composition of  $3\text{Cu}_2\text{S}\cdot 2\text{Bi}_2\text{S}_3$  to copper-bismuth sulfide mineral from the Daniel mine, Wittichen, Baden which occurred with chalcopyrite and native bismuth in barite, usually in needle-like crystal. They named it klaprothite. Murdoch<sup>3)</sup> concluded that the validity of the species was very doubtful in 1916. Schneiderhöhn and Ramdohr<sup>4)</sup> (1931) recognized klaprothite, considering Murdoch's decision incorrect, but Short<sup>5)</sup> (1940) had a doubt about it. Moreover, while it was again described in Dana's System of Mineralogy<sup>6)</sup> (1944) as a well defined mineral species with orthorhombic form, Nuffield<sup>7)</sup> (1947) minutely investigated the specimens by means of X-ray powder photograph and found that they were wittichenite, emplectite, tetrahedrite, or their mixture. However, Ramdohr<sup>8)</sup> still suggested a possibility of existence of klaprothite in his new book.

On the other hand, cuprobismutite, found by Hillebrand<sup>9)</sup> from the Missouri mine, Hall's Valley, Park Country, Colorado in 1884, was given first  $3(\text{Cu}, \text{Ag})_2\text{S}\cdot 4\text{Bi}_2\text{S}_3$  of chemical composition by him. The Hillebrand's data were described in the Dana's System of Mineralogy<sup>10)</sup> (1892), and Schneiderhöhn and Ramdohr<sup>4)</sup> reported another occurrence from Arnsberg, Westphalis, but Short<sup>5)</sup> and Palache<sup>11)</sup> (1940) afterwards decided that these specimens were emplectite or the mixture of emplectite and bismuthinite, and denied the existence of cuprobismutite. From the results of re-examination on the type specimens from Missouri mine, however, Nuffield<sup>12)</sup> (1952) identified cuprobismutite as valid species with chemical composition of  $\text{Cu}_2\text{S}\cdot\text{Bi}_2\text{S}_3$ , and suggested dimorphic relations with emplectite.

Some experimental investigations of this system have been done. Gaudin and Dicke<sup>13)</sup> (1939) synthesized artificially Phase A ( $\text{Cu}_2\text{S}\cdot 2\text{Bi}_2\text{S}_3$ ), Phase B ( $3\text{Cu}_2\text{S}\cdot 2\text{Bi}_2\text{S}_3$ ), and Phase C ( $3\text{Cu}_2\text{S}\cdot\text{Bi}_2\text{S}_3$ ), and reported that they respectively corresponded to cuprobismutite, klaprothite and wittichenite, but the experi-

\* Department of Mining and Mineral Engineering.

ments were carried on in the air and the atomic ratio of these phases does not seem very accurate. Nuffield<sup>7)</sup> succeeded in synthesizing wittichenite from the Cu-Bi-S melt, but failed in synthesizing klaprothite and emplectite. He also described<sup>12)</sup> a new synthetic phase  $3\text{Cu}_2\text{S}\cdot 5\text{Bi}_2\text{S}_3$  and a homogeneous phase which has similar X-ray powder pattern of cuprobismutite are produced from the melt. The authors<sup>14)</sup> described four synthetic phases of the system, wittichenite, cuprobismutite,  $\text{Cu}_3\text{Bi}_5\text{S}_9$  and  $\text{CuBi}_3\text{S}_5$  in 1965. Recently Buhlmann<sup>15)</sup> (1971) investigated this system and gave a short paper on the phase relation of this binary system. He does not mention his experiments much in detail but shows only one phase diagram. His result shown in the diagram is almost similar to ours except some of the temperatures of phase changes and detail parts.

### Experimental Procedures

#### *Starting Materials:*

The primary starting materials used in this experiments were electrolytic copper of 99.99+ % in purity, bismuth metal of 99.9+ % in purity, and crystalline sulfur refined as guaranteed reagent by Kanto Chemical Co., purity grade 99.98+ %. Copper chips were reduced in hydrogen atmosphere at about 900°C for 2 hours prior to experiments. Using these elements the end-members of the system,  $\text{Cu}_2\text{S}$  and  $\text{Bi}_2\text{S}_3$  were synthesized first in evacuated silica glass tube and then they were used as starting materials for the phase equilibrium study of the binary system.

#### *Method of Synthesis:*

Detailed technique of the synthesis has been described in the preceding paper<sup>16)</sup>. Carefully weighed amounts of the previously prepared compound,  $\text{Cu}_2\text{S}$  and  $\text{Bi}_2\text{S}_3$  were sealed into evacuated silica glass or Hario hard glass tube. By inserting a closely fitting glass rod into the tubes, the vapor volume was effectively reduced as described by Kullerud and Yorder<sup>17)</sup>. Tubes thus prepared were heated in horizontal or vertical furnaces for various periods and at desired temperatures, controlled within  $\pm 1^\circ\text{C}$  or  $\pm 3^\circ\text{C}$ , depending on the requirement of the experiment. When required, the individual samples were repeatedly ground under acetone and re-heated at a given temperature two or three times to attain equilibrium. Every weighing was performed on an analytical balance, permitting an accuracy of  $\pm 0.05$  mg per weighing. The uncertainty in the composition never exceeded 0.1 wt% and was less than 0.05 wt% in most runs. All the runs performed in this study were quenched. The tubes were dropped into ice water and then could be lowered from the furnace temperature to the room temperature in less than 3 seconds.

#### *Identification of Phases:*

The reaction products of the experiments were routinely identified at room temperature by reflecting microscope and X-ray powder diffractometer. A

small quantity of the products, generally in powder or sintered mass, were mounted on polyester resin Rigorac and polished smoothly, and then examined under the microscope. Generally, as optical properties of each cuprobismuth sulfide phases are quite similar, they are hardly identified one another, but microscopic observation was useful to determine homogeneity of products.

The products obtained in all experiments were identified mainly by careful examination of their X-ray powder diffraction patterns. When measurements of d-spacing in high accuracy were required, high purity silicon (99.9999%) was used as an internal standard. Rigaku X-ray diffractometer, Geigerflex was employed in all cases. In some cases, high temperature X-ray technique and single crystal methods were employed. High temperature studies were conducted within nitrogen atmosphere by using Rigaku high temperature X-ray diffractometer and Rigaku continuous cassette moving high temperature camera.

*The Differential Thermal Analysis:*

The differential thermal analysis (DTA) was very useful for a phase study, especially to know easily the temperature of any phase changing reactions. The apparatus and methods have been described before in detail.<sup>18)</sup> All analyses were performed in the evacuated silica glass tubes each having a thermocouple-well of about 5 mm depth at the bottom of the tube. The similar techniques have been used by Jensen<sup>19)</sup>, Kracek<sup>20)</sup>, Kullerud and Yund<sup>21)</sup>, Dunne and Kerr<sup>22)</sup>, and Moh<sup>23)</sup>. In order to check the accuracy of the apparatus and to make a calibration curve to correct the reaction temperature,

Table 1. Calibration of the D.T.A. by melting points of metals

Metal	Melting point (°C)	Heating rate	Temp. at peak beginning (°C)	Deviation (°C)	Cooling analysis (°C)
Tin	231.9	1.25°/min.	233	+1.1	211
		5°/min.	235	+3.1	
		10°/min.	235	+3.1	
Bismuth	271.0	1.25°/min.	271	±0.0	272
		5°/min.	272	+1.0	
		10°/min.	273	+2.0	
Lead	327.3	1.25°/min.	329	+1.7	331
		5°/min.	330	+2.7	
		10°/min.	331	+3.7	
Zinc	419.7	1.25°/min.	421	+1.3	421
		5°/min.	421	+1.3	
		10°/min.	422	+2.3	
Antimony	630.5	1.25°/min.	631	+0.5	571
		10°/min.	632	+1.5	
Aluminium	660.1	1.25°/min.	661	+0.9	660
		5°/min.	663	+2.9	
		10°/min.	664	+3.9	

Table 2. Results of experimental runs at 500°C and 400°C

Cu <sub>2</sub> S mol%	Temp. (°C)	Time (days)	Products
100.0	500	5	Cu <sub>2</sub> S ss
90.0	500	5	Cu <sub>9</sub> BiS <sub>6</sub> ss
85.0	500	5	Cu <sub>9</sub> BiS <sub>6</sub> ss
85.0	500	5	Cu <sub>9</sub> BiS <sub>6</sub> ss
82.5	500	5	Cu <sub>9</sub> BiS <sub>6</sub> ss
80.0	500	5	Cu <sub>9</sub> BiS <sub>6</sub> ss + Cu <sub>3</sub> BiS <sub>3</sub> ss
75.0	500	5	Cu <sub>9</sub> BiS <sub>6</sub> ss + (Cu <sub>3</sub> BiS <sub>3</sub> ss)
73.0	500	5	Cu <sub>3</sub> BiS <sub>3</sub> ss
70.0	500	5	Cu <sub>3</sub> BiS <sub>3</sub> ss + Cu <sub>3</sub> Bi <sub>5</sub> S <sub>9</sub> ss
60.0	500	5	Cu <sub>3</sub> BiS <sub>3</sub> ss + Cu <sub>3</sub> Bi <sub>5</sub> S <sub>9</sub> ss
50.0	500	5	Cu <sub>3</sub> BiS <sub>3</sub> ss + Cu <sub>3</sub> Bi <sub>5</sub> S <sub>9</sub> ss
40.0	500	5	Cu <sub>3</sub> Bi <sub>5</sub> S <sub>9</sub> ss
37.5	500	5	Cu <sub>3</sub> Bi <sub>5</sub> S <sub>9</sub> ss
30.0	500	5	Cu <sub>3</sub> Bi <sub>5</sub> S <sub>9</sub> ss + CuBi <sub>3</sub> S <sub>5</sub>
25.0	500	5	CuBi <sub>3</sub> S <sub>5</sub>
20.0	500	5	CuBi <sub>3</sub> S <sub>5</sub> + Bi <sub>2</sub> S <sub>3</sub>
5.0	500	5	CuBi <sub>3</sub> S <sub>5</sub> + Bi <sub>2</sub> S <sub>3</sub>
0.0	500	5	Bi <sub>2</sub> S <sub>3</sub>
100.0	400	14	Cu <sub>2</sub> S ss
90.0	400	14	Cu <sub>9</sub> BiS <sub>6</sub> ss
87.5	400	14	Cu <sub>9</sub> BiS <sub>6</sub> ss + Cu <sub>3</sub> BiS <sub>3</sub> ss
85.0	400	14	Cu <sub>9</sub> BiS <sub>6</sub> ss + Cu <sub>3</sub> BiS <sub>3</sub> ss
80.0	400	14	Cu <sub>9</sub> BiS <sub>6</sub> ss + Cu <sub>3</sub> BiS <sub>3</sub> ss
75.0	400	14	Cu <sub>3</sub> BiS <sub>3</sub> ss
60.0	400	14	Cu <sub>3</sub> BiS <sub>3</sub> ss + Cu <sub>24</sub> Bi <sub>26</sub> S <sub>51</sub>
50.0	400	14	Cu <sub>24</sub> Bi <sub>26</sub> S <sub>51</sub> (+ Cu <sub>3</sub> BiS <sub>3</sub> ss)
48.0	400	14	Cu <sub>24</sub> Bi <sub>26</sub> S <sub>51</sub>
42.9	400	14	Cu <sub>24</sub> Bi <sub>26</sub> S <sub>51</sub> + CuBi <sub>3</sub> S <sub>5</sub>
37.5	400	14	Cu <sub>24</sub> Bi <sub>26</sub> S <sub>51</sub> + CuBi <sub>3</sub> S <sub>5</sub>
30.0	400	14	Cu <sub>24</sub> Bi <sub>26</sub> S <sub>51</sub> + CuBi <sub>3</sub> S <sub>5</sub>
25.0	400	14	CuBi <sub>3</sub> S <sub>5</sub>
20.0	400	14	CuBi <sub>3</sub> S <sub>5</sub> + Bi <sub>2</sub> S <sub>3</sub>

Table 3. Stable crystalline phases in the Cu<sub>2</sub>S–Bi<sub>2</sub>S<sub>3</sub> system

Phases (Composition)	Cu <sub>2</sub> S mol%	Minerals
Cu <sub>2</sub> S	100.0	chalcocite
Cu <sub>9</sub> BiS <sub>6</sub> (9Cu <sub>2</sub> S·Bi <sub>2</sub> S <sub>3</sub> )	90.0	
Cu <sub>3</sub> BiS <sub>3</sub> (3Cu <sub>2</sub> S·Bi <sub>2</sub> S <sub>3</sub> )	75.0	wittichenite
Cu <sub>24</sub> Bi <sub>26</sub> S <sub>51</sub> (48Cu <sub>2</sub> S·52Bi <sub>2</sub> S <sub>3</sub> )	48.0	{cuprobismutite }emphlectite
Cu <sub>3</sub> Bi <sub>5</sub> S <sub>9</sub> (3Cu <sub>2</sub> S·5Bi <sub>2</sub> S <sub>3</sub> )	37.5	
CuBi <sub>3</sub> S <sub>5</sub> (Cu <sub>2</sub> S·3Bi <sub>2</sub> S <sub>3</sub> )	25.0	
Bi <sub>2</sub> S <sub>3</sub>	0.0	bismuthinite

pure metals such as tin(Sn), bismuth(Bi), lead(Pb), zinc(Zn), antimony(Sb), and aluminum(Al) were used as an external standard, and the results are shown in Table 1. They show clearly that melting temperatures given from the DTA curves were fairly in good agreement with true melting points of the metals. When the heating rate of the analysis is so slow as  $1.25^\circ\text{C}/\text{min.}$  or less and the observed temperature is corrected to  $1^\circ\text{C}$  lower after the analysis, the accuracy of the reaction temperature measured by the DTA was within  $\pm 1^\circ\text{C}$  for melting of metals. The best results were obtained in our experiment of this system when the heating rates were  $0.6^\circ\text{C}$  and  $1.25^\circ\text{C}$  per minute and the accuracy would be within  $\pm 3^\circ\text{C}$ . Besides, if more than one reaction occur within a narrow temperature range on heating, the reaction peaks will overlap in the high heating rate analysis. However, the analysis with the low heating rate may separate individual reactions and facilitate to read the reaction temperatures from the DTA curves. Though Zakjarov<sup>24)</sup> described the small effect of the sample mass, Shima<sup>25)</sup> could not find any effect on the result in the analyses of the sample mass of 0.2 to 1.0 g. The routine analyses were done on the sample of 0.2 to 0.5 g.

### Experimental Results

#### *Preliminary Synthesis of Phases:*

The primary purpose of this study was to synthesize all stable phases in the  $\text{Cu}_2\text{S}-\text{Bi}_2\text{S}_3$  system because of the contradictory results reported by earlier workers. Next, the compositional and thermal stability field of each phases was determined and the phase relations of the system such as solidus and liquidus relations were investigated. Experiments by quenching methods at  $500^\circ\text{C}$  and  $400^\circ\text{C}$  were made preliminary to establish the stable phases of the system.

The experimental results of the runs are compiled in Table 2. Though in the table nothing is mentioned about vapor phase, these solid phases always keep equilibrium with sulfur vapor under their own sulfur vapor pressure.

As shown in the table six condensed phases of  $\text{Cu}_2\text{S}$ ,  $\text{Cu}_9\text{BiS}_6$ ,  $\text{Cu}_3\text{BiS}_3$ ,  $\text{Cu}_3\text{Bi}_5\text{S}_9$ ,  $\text{CuBi}_3\text{S}_5$ , and  $\text{Bi}_2\text{S}_3$  are stable at  $500^\circ\text{C}$  in the binary join, and at  $400^\circ\text{C}$  in addition to these six,  $\text{Cu}_{24}\text{Bi}_{26}\text{S}_{51}$  becomes stable while  $\text{Cu}_3\text{Bi}_5\text{S}_9$  becomes unstable. The seven stable crystalline phases given in Table 3 are all entirely homogeneous under the ore microscope and their optical properties were already reported.<sup>14) 15)</sup>  $\text{Cu}_2\text{S}$ ,  $\text{Cu}_3\text{BiS}_3$ ,  $\text{Cu}_{24}\text{Bi}_{26}\text{S}_{51}$ , and  $\text{Bi}_2\text{S}_3$  correspond to chalcocite, wittichenite, cuprobismutite, and bismuthinite respectively, but other three binary compounds have not been found in nature up to date. The X-ray powder diffraction data of four binary phases,  $\text{Cu}_3\text{BiS}_3$ ,  $\text{Cu}_{24}\text{Bi}_{26}\text{S}_{51}$ ,  $\text{Cu}_3\text{Bi}_5\text{S}_9$ ,  $\text{CuBi}_3\text{S}_5$  are shown in Tables 4, 5, 6 and 7. As is evident from the Tables 4 and 5, the data of  $\text{Cu}_3\text{BiS}_3$  and  $\text{Cu}_{24}\text{Bi}_{26}\text{S}_{51}$  are in good agreement with those of natural wittichenite and cuprobismutite by Nuffield<sup>7)</sup> and Berry and Thompson<sup>26)</sup> respectively. Klaprothite,  $\text{Cu}_6\text{Bi}_4\text{S}_9$ , and dognacskite,  $\text{Cu}_2\text{Bi}_4\text{S}_7$  were not stable phases in the system at  $400^\circ\text{C}$  and  $500^\circ\text{C}$ .

Table 4. The data of X-ray powder diffraction for synthetic  $\text{Cu}_3\text{BiS}_3$  (wittichenite).

(1)		(2)		
d	I	d	I	hkl
5.66	20	5.68	1	011
5.22	20	5.22	1	020
4.55	55	4.55	4	111
3.85	45	3.83	1	200
3.62	15	3.62	1	121, 210
3.35	20	3.34	1	002, 201
3.18	50	3.19	3	012, 211
3.08	80	3.08	8	220, 102, 031
2.95	35	2.96	1	112
2.86	100	2.85	10	131
2.814	25	2.81	1/2	022
2.648	50	2.66	4	122
2.604	15			
2.578	25	2.58	2	040, 230
2.492	5	2.49	1/2	310
2.401	20	2.39	3	032, 231, 301
2.338	10	2.34	1/2	311
2.301	7	2.28	1/2	141, 320, 132
2.275	2			
2.181	10	2.17	2	013, 321
2.104	5	2.10	1/2	113
2.051	15	2.05	2	330, 023, 042
2.038	10			241
1.997	25	1.989	2	312, 150
1.987	15			123
1.929	10	1.910	1/2	151
1.886	20	1.895	3	322
1.824	30	1.821	3	113, 250
1.812	10			
1.765	25	1.762	3	052

(1) Synthetic  $\text{Cu}_3\text{BiS}_3$ (2) X-ray powder data for wittichenite by Nuffield<sup>7)</sup>

Table 5. The data of X-ray powder diffraction for synthetic  $\text{Cu}_{24}\text{Bi}_{26}\text{S}_{51}$ 

(1)		(2)		
d	I	d	I	hkl
8.22	7			
6.92	9			
6.29	40	6.24	2	$\bar{2}02$
5.63	8			
5.01	25			
4.55	15			
4.37	20			
4.31	25	4.31	3	400
3.85	12			
3.71	50			
3.63	85	3.65	4	111, $\bar{4}03$
3.46	40	3.47	1	402, $\bar{1}12$
3.34	5			
3.11	80	3.23	4	310, $\bar{3}11$ , 204
3.17	10			
3.10	100	3.10	10	311, $\bar{1}13$ , $\bar{3}12$
3.02	12			
3.00	30			
2.94	10	2.96	1/2b	113, $\bar{6}01$
2.92	25			
2.866	40	2.86	1b	$\bar{6}02$ , 312, $\bar{3}13$
2.731	40	2.73	6	601, $\bar{6}03$ , 405
2.645	15			
2.589	12			
2.564	12	2.58	1	$\bar{3}14$ , $\bar{5}12$
2.528	10			
2.492	12	2.49	1/2	511, 006
2.443	5			
2.405	12	2.49	1/2	
2.328	7			
2.307	20	2.30	1/2	$\bar{6}05$ , 206
2.176	50	2.17	2	$\bar{2}07$ , 800
2.132	15			
2.113	12			
2.092	25	2.09	2	710, 801, $\bar{6}06$
2.049	10	2.00	1/2	207, 802
1.959	20	1.961	3	020, $\bar{7}14$
1.943	10			
1.923	9			
1.897	9			

(1) Synthetic  $\text{Cu}_{24}\text{Bi}_{26}\text{S}_{51}$  (cuprobimutite)(2) Data for natural cuprobismutite by Berry and Thompson<sup>27)</sup>

Table 6. The data of X-ray powder diffraction for synthetic  $\text{Cu}_3\text{Bi}_5\text{S}_9$ .

d (meas.)	I	hkl	d (calc.)
7.26	5	002	7.26
6.51	8	200	6.50
6.35	7	$\bar{2}01$	6.37
5.61	18	201	5.58
5.33	5	$\bar{2}02$	5.34
4.49	23	202	4.47
3.84	8	110	3.81
3.63	20	$\left\{ \begin{array}{l} 111 \\ 004 \end{array} \right.$	$\left\{ \begin{array}{l} 3.64 \\ 3.63 \end{array} \right.$
3.60	65	203	3.59
3.467	100	$11\bar{2}$	3.445
3.429	65	$20\bar{4}$	3.440
3.295	30	$\left\{ \begin{array}{l} 112 \\ 401 \end{array} \right.$	$\left\{ \begin{array}{l} 3.302 \\ 3.299 \end{array} \right.$
3.251	7	400	3.251
3.176	18	$40\bar{2}$	3.184
3.059	10	401	3.059
2.950	50	$\left\{ \begin{array}{l} 204 \\ 310 \\ 113 \end{array} \right.$	$\left\{ \begin{array}{l} 2.956 \\ 2.931 \\ 2.920 \end{array} \right.$
2.905	11	005	2.905
2.825	80	$\left\{ \begin{array}{l} 20\bar{5} \\ 31\bar{2} \\ 311 \end{array} \right.$	$\left\{ \begin{array}{l} 2.846 \\ 2.839 \\ 2.809 \end{array} \right.$
2.657	17	$\left\{ \begin{array}{l} 40\bar{4} \\ 31\bar{3} \end{array} \right.$	$\left\{ \begin{array}{l} 2.667 \\ 2.652 \end{array} \right.$
2.501	12	$\left\{ \begin{array}{l} 403 \\ 205 \end{array} \right.$	$\left\{ \begin{array}{l} 2.502 \\ 2.494 \end{array} \right.$
2.264	35	115	2.254
2.178	9	$51\bar{2}$	2.176
2.106	25	$\left\{ \begin{array}{l} 60\bar{3} \\ 511 \end{array} \right.$	$\left\{ \begin{array}{l} 2.123 \\ 2.108 \end{array} \right.$
2.100	25	$51\bar{3}$	2.105
2.094	25	$\left\{ \begin{array}{l} 11\bar{6} \\ 601 \end{array} \right.$	$\left\{ \begin{array}{l} 2.092 \\ 2.090 \end{array} \right.$
2.077	13	007	2.076
2.011	35	$\left\{ \begin{array}{l} 60\bar{4} \\ 512 \end{array} \right.$	$\left\{ \begin{array}{l} 2.025 \\ 2.006 \end{array} \right.$
2.002	35	$\left\{ \begin{array}{l} 51\bar{4} \\ 405 \\ 116 \end{array} \right.$	$\left\{ \begin{array}{l} 2.002 \\ 1.998 \\ 1.997 \end{array} \right.$
1.987	25	$\left\{ \begin{array}{l} 31\bar{6} \\ 602 \end{array} \right.$	$\left\{ \begin{array}{l} 1.987 \\ 1.983 \end{array} \right.$
1.866	25		



Table 7. The data of X-ray powder diffraction for synthetic  $\text{CuBi}_3\text{S}_5$ 

d (meas.)	I	hkl	d (calc.)
6.63	1	20 $\bar{1}$	6.62
6.36	4	002	6.36
5.98	11	200	5.96
5.78	4	20 $\bar{2}$	5.78
4.68	25	201	4.68
4.24	3	003	4.24
3.82	4	011	3.83
3.64	40	202	3.64
3.50	100	20 $\bar{4}$	3.51
3.305	25	40 $\bar{2}$	3.307
3.179	15	004	3.179
3.166	10	40 $\bar{3}$	3.170
3.093	10	112	3.085
2.983	40	400	2.983
2.962	10	31 $\bar{1}$	2.960
2.831	55	{310 20 $\bar{5}$ }	2.828 2.822
2.783	5	31 $\bar{3}$	2.780
2.661	5	{401 113}	2.660 2.657
2.536	10	005	2.543
2.406	5	204	2.406
2.339	5	{20 $\bar{6}$ 402}	2.343 2.339
2.291	25	114	2.290
2.266	3	11 $\bar{5}$	2.265
2.243	3	40 $\bar{6}$	2.248
2.120	30	006	2.120
2.110	25	60 $\bar{1}$	2.109
2.055	10	{510 403}	2.052 2.056
2.020	15	31 $\bar{6}$	2.021
2.014	20	020	2.010
2.001	15	51 $\bar{5}$	2.003
1.996	10	20 $\bar{7}$	1.995
1.988	10	{600 021}	1.989 1.985
1.972	9	40 $\bar{7}$	1.978
1.918	17	222	1.917
1.848	9		
1.819	3		
1.763	5		
1.747	11		
1.719	5		

*Results of the Differential Thermal Analysis:*

In order to determine the temperature of the phase changing reactions and to construct the binary phase diagram roughly, the DTA were carried out on each of the seven condensed phases and on the mixtures of neighbouring two

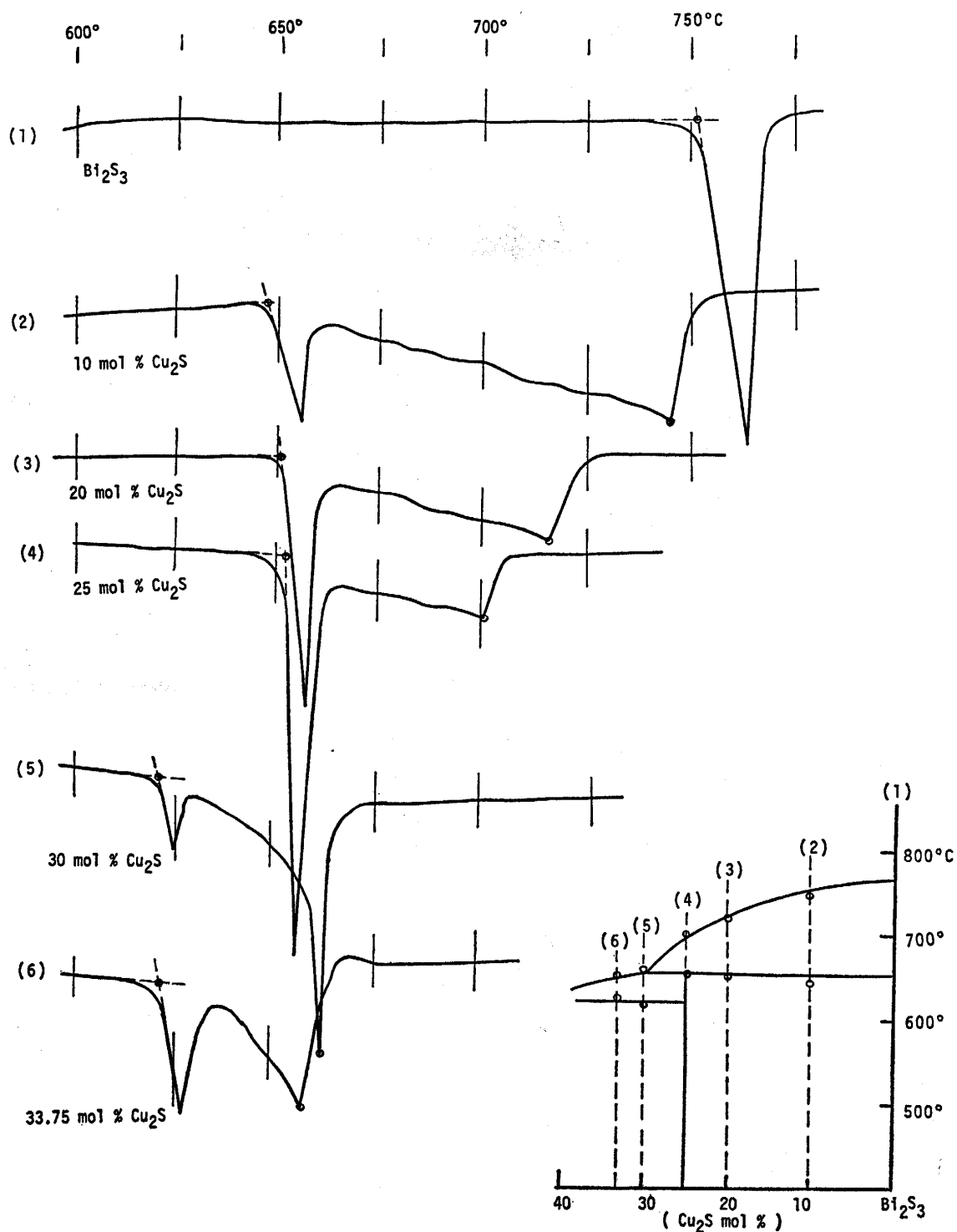


Fig. 1. The DTA curves and schematic phase diagram of the  $\text{Cu}_2\text{S}$ - $\text{Bi}_2\text{S}_3$  system (1)

phases which have various bulk compositions. Because of the supercooling phenomena, recorded temperatures of the thermal effects on cooling analysis are usually considerably lower than the true equilibrium temperatures in this system as well as in the system including antimony. As discussed before satisfactory results were given by the heating analysis with rather low heating rate in this system. The results and the schematic phase diagram models expected from the DTA curves are shown in the four figures, 1, 2, 3, and 4.

Fig. 1 shows six DTA curves performed on the samples containing less than 35 percent in  $\text{Cu}_2\text{S}$  molecule. Curve (1) and curve (4) are experiments on condensed homogeneous phases of  $\text{Bi}_2\text{S}_3$  and  $\text{CuBi}_3\text{S}_5$  respectively, and the former shows congruent melting effect at  $756^\circ\text{C}$ . Each five curves except one for  $\text{Bi}_2\text{S}_3$  has an endothermic peak with two steps but they are clearly divided into two groups. Curves (2), (3), and (4) of the first group show nearly the same beginning temperature of the first endothermic peaks around  $650^\circ\text{C}$  which

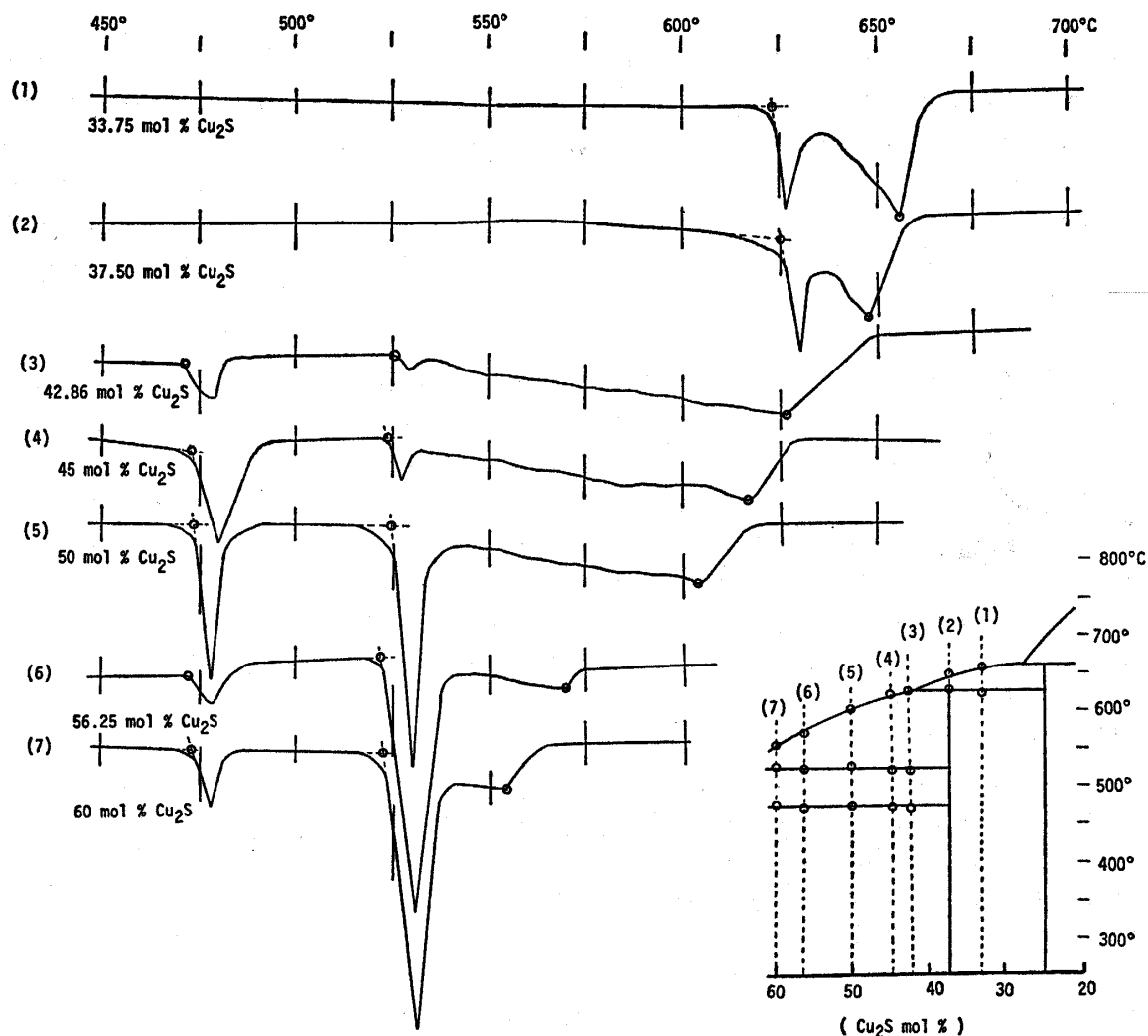


Fig. 2. The DTA curves and schematic phase diagram of the  $\text{Cu}_2\text{S}-\text{Bi}_2\text{S}_3$  system (2)

indicate the incongruent melting of  $\text{CuBi}_3\text{S}_5$ , and they intersect the liquidus at  $743^\circ\text{C}$ ,  $714^\circ\text{C}$ , and  $697^\circ\text{C}$  respectively. Other two runs containing 30.0 mol% and 33.75 mol%  $\text{Cu}_2\text{S}$ , curves (5) and (6), show the thermal effects at  $618^\circ\text{C}$  and  $620^\circ\text{C}$  which indicate the incongruent melting of the condensed phase  $\text{Cu}_3\text{Bi}_5\text{S}_9$ , and the bottom points of the second peaks,  $659^\circ\text{C}$  and  $658^\circ\text{C}$ , represent the completion of melting in their compositions.

The results of the run between 60 mol % and 33 mol %  $\text{Cu}_2\text{S}$  are shown in Fig. 2. The first two runs in the figure, curves (1) and (2), show the similar curves each other, one was performed on the mixture of  $\text{CuBi}_3\text{S}_5$  and  $\text{Cu}_3\text{Bi}_5\text{S}_9$  and the other was on stoichiometric composition of  $\text{Cu}_3\text{Bi}_5\text{S}_9$ , both synthesized at  $500^\circ\text{C}$  for 120 hours. The beginning temperatures of the first thermal effect,  $620^\circ\text{C}$  and  $623^\circ\text{C}$ , correspond to the incongruent melting of  $\text{Cu}_3\text{Bi}_5\text{S}_9$ . Curves (3) and (4) in Fig. 2 are the results for the experiments on mixtures of  $\text{Cu}_{24}\text{Bi}_{26}\text{S}_{51}$  and  $\text{Cu}_3\text{Bi}_5\text{S}_9$ , and (5), (6), and (7), on mixtures of  $\text{Cu}_3\text{BiS}_3$  and  $\text{Cu}_{24}\text{Bi}_{26}\text{S}_{51}$ , synthesized at  $500^\circ\text{C}$  and then annealed at  $300^\circ\text{C}$  for 21 days. Each curves have two distinct endothermic peaks and a following wide spread peak with gentle slope. The lower sharp peaks begin at the nearly the same temperature of  $474 \pm 4^\circ\text{C}$  and the intensity of the peaks becomes weaker as the bulk composition is away far from 50.0 mol%  $\text{Cu}_2\text{S}$ . These peaks correspond to breakdown of  $\text{Cu}_{24}\text{Bi}_{26}\text{S}_{51}$  into  $\text{Cu}_3\text{BiS}_3$  and  $\text{Cu}_3\text{Bi}_5\text{S}_9$ . Eutectic melting of them are indicated by the beginning of the second sharp endothermic peaks at about  $523^\circ\text{C}$  and liquidus temperatures, represented on the end-point of the last wide spread endothermic peaks, become lower smoothly like  $626^\circ\text{C}$ ,  $618^\circ\text{C}$ ,  $602^\circ\text{C}$ ,  $569^\circ\text{C}$ , and  $553^\circ\text{C}$  as increase  $\text{Cu}_2\text{S}$  molecule in the bulk composition.

Fig. 3 shows six DTA curves, five of them performed on mixtures of  $\text{Cu}_3\text{BiS}_3$  and  $\text{Cu}_{24}\text{Bi}_{26}\text{S}_{51}$  and one on stoichiometric  $\text{Cu}_3\text{BiS}_3$  which were synthesized at  $500^\circ\text{C}$  and annealed at  $300^\circ\text{C}$  for 21 days. The bulk composition of the samples are 60.0 mole%, 63.75 mol%, 67.5 mol%, 71.25 mol%, 73.03 mol%, and 75.0 mol%  $\text{Cu}_2\text{S}$ . These DTA curves, especially, curves (3), (4), and (5) are very difficult to interpret because complicate reactions occur successively within a narrow temperature range. Although the decomposition effect of  $\text{Cu}_{24}\text{Bi}_{26}\text{S}_{51}$  is observed in the five curves except the run containing 75.0 mol%  $\text{Cu}_2\text{S}$ , the intensity of the peaks of this reaction decrease extremely in curves (4) and (5), because of the small quantity of the phase  $\text{Cu}_{24}\text{Bi}_{26}\text{S}_{51}$ . Liquidus temperatures come closer to the beginning temperature of melting according as bulk composition comes near the eutectic point, then the eutectic point of  $\text{Cu}_3\text{BiS}_3$  and  $\text{Cu}_3\text{Bi}_5\text{S}_9$  is expected to situate at the composition between 67.5 mol% and 63.75 mol%  $\text{Cu}_2\text{S}$  from the curves. Experiment of the stoichiometric composition of  $\text{Cu}_3\text{BiS}_3$  is shown as curve (6) in Fig. 4, showing incongruent melting, however as mention below, the compositional range of  $\text{Cu}_3\text{BiS}_3$  solid solution shifts successively towards less  $\text{Cu}_2\text{S}$  molecule on heating, then the beginning of the endothermic peak is not sharp.

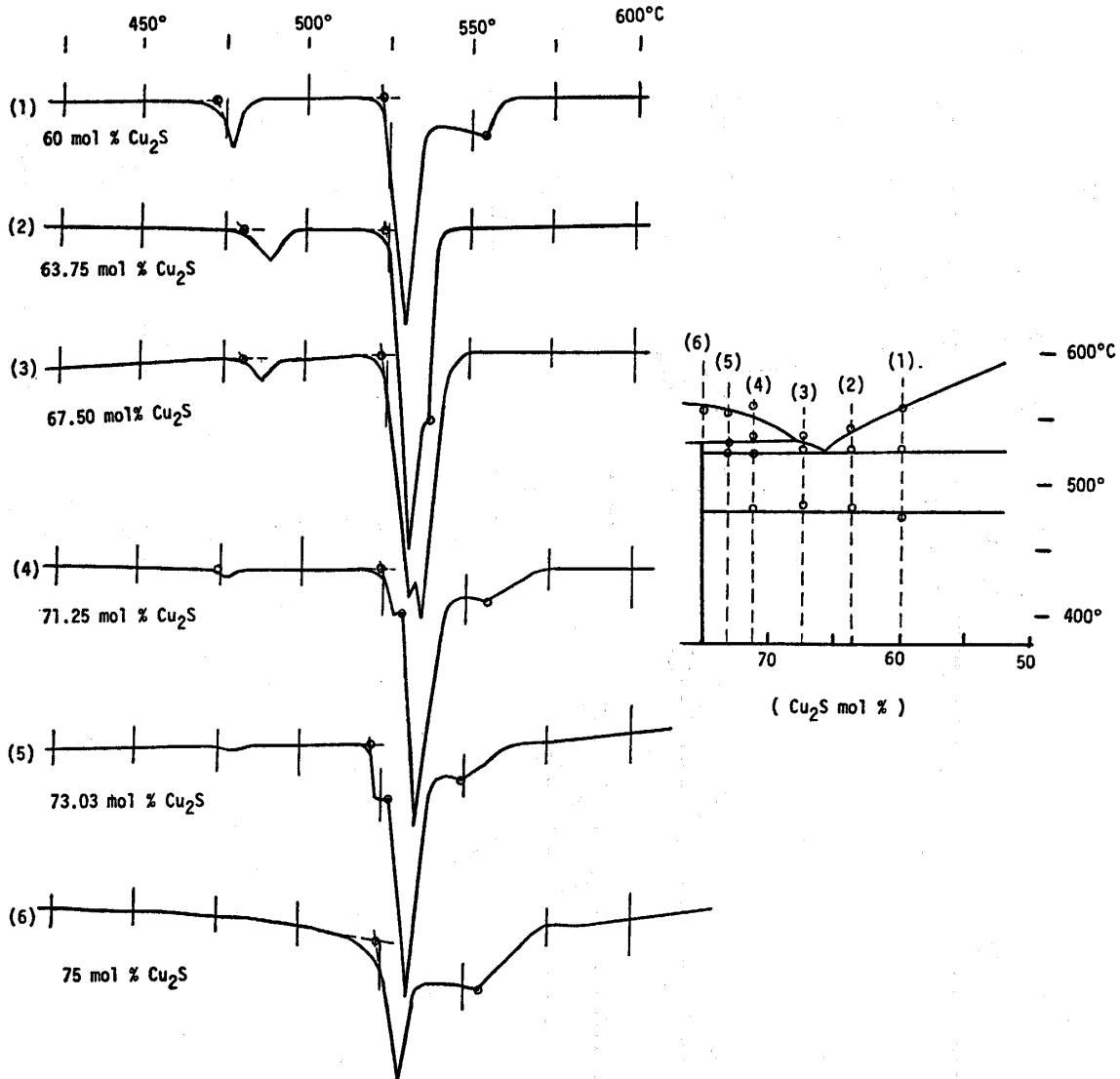


Fig. 3. The DTA curves and schematic phase diagram of the  $\text{Cu}_2\text{S}-\text{Bi}_2\text{S}_3$  system (3)

Fig. 4 shows the experimental results for bulk compositions of 77.5 mol%, 80.0 mol%, and 85.0 mol%  $\text{Cu}_2\text{S}$ . Before the analysis, sample synthesized at  $500^\circ\text{C}$  were annealed at  $300^\circ\text{C}$  at least for 20 days and then the starting sample consists of  $\text{Cu}_2\text{S}$  solid solution and  $\text{Cu}_3\text{BiS}_3$ . Their heating analysis curves are characterized by extremely gentle endothermic reactions which suggest thermal reaction accompanying with increasing temperature such as solid solution reaction. For example, the experiment containing 77.5 mol%  $\text{Cu}_2\text{S}$  shows very gentle endothermic reaction from about  $400^\circ\text{C}$  on heating which suggested that  $\text{Cu}_3\text{BiS}_3$  molecule solves gradually into  $\text{Cu}_9\text{BiS}_6$  solid solution. The reaction completes at  $525^\circ\text{C}$ , meaning solvus, and then the solid solution begins to melt at about  $535^\circ\text{C}$ , showing again a gentle endothermic peak from this temperature on the DTA curve. Liquidus is intersected at about  $564^\circ\text{C}$ . As the compositions come closer to  $\text{Cu}_2\text{S}$  the solvus, indicated at the point of the bottom of the

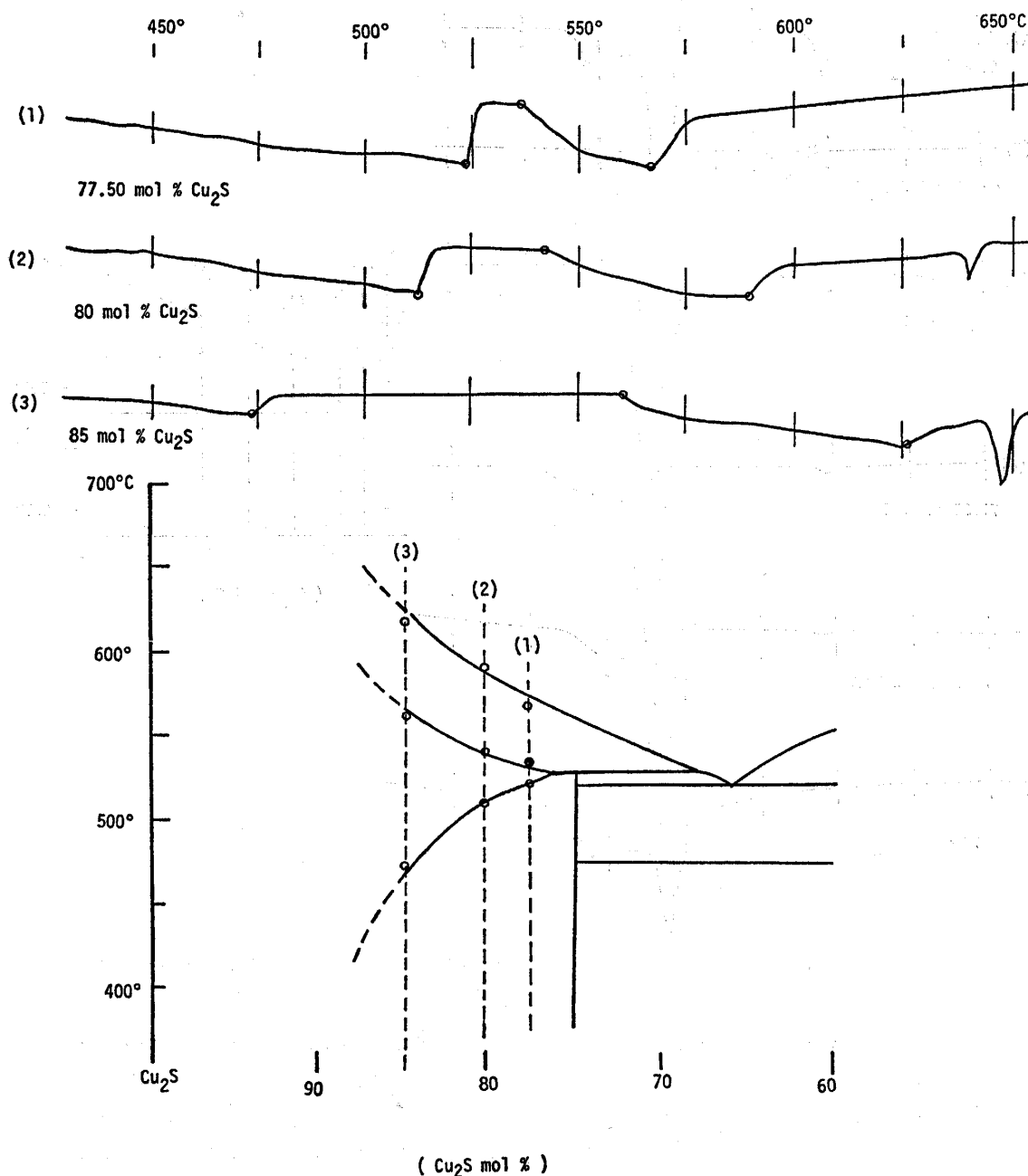


Fig. 4. The DTA curves and schematic phase diagram of the  $\text{Cu}_2\text{S}$ - $\text{Bi}_2\text{S}_3$  system (4)

first gentle peak, becomes lower and lower as 525°C, 511°C, and 473°C, while the solidus, represented as the beginning point of the second gentle peak, becomes higher and higher like 535°C, 539°C, and 578°C.

Results of twenty thermal analyses are summarized in Table 8.

Table 8. Results of the differential thermal analysis for the  $\text{Cu}_2\text{S}-\text{Bi}_2\text{S}_3$  system

$\text{Cu}_2\text{S}$ mol%	$T_1$	$T_2$	$T_3$	$T_4$	$T_5$	$T_6$	$T_7$	$T_8$
0.00	756°C							
10.00	743	648°C						
20.00	714	649						
25.00	697	651						
30.00	659		618°C					
33.75	658		620					
37.50	647		623					
42.50	626				525°C	470°C		
45.00	618				523	471		
50.00	602				524	473		
56.25	569				523	470		
60.00	553				523	474		
63.75	536				525	478		
67.50	535				524	478		
71.25	552			530°C	521	475		
73.03	547			526				
75.00	551			524				
77.50	563						535°C	525°C
80.00	588						539	511
85.00	626						578	473
mean value		649°C	620°C	527°C	523°C	474°C		

$T_1$ : Liquidus

$T_2$ : Incongruent of  $\text{CuBi}_3\text{S}_5$

$T_3$ : Incongruent of  $\text{Cu}_3\text{Bi}_5\text{S}_9$

$T_4$ : Incongruent of  $\text{Cu}_3\text{BiS}_3$

$T_5$ : Eutectic of  $\text{Cu}_3\text{BiS}_3-\text{Cu}_3\text{Bi}_5\text{S}_9$

$T_6$ : Decomposition of  $\text{Cu}_{24}\text{Bi}_{26}\text{S}_{51}$

$T_7$ : Solidus of  $\text{Cu}_9\text{BiS}_6$

$T_8$ : Solvus of  $\text{Cu}_9\text{BiS}_6$

#### Quenching Experiments for Phase Relations:

Since the DTA is essentially on the dynamic analysis, it does not theoretically represent the true equilibrium relations. Then it is necessary to examine the results of the DTA study critically by means of the other method. Several quenching and additional investigations are performed.

*Determination of Some Melting Relations:* In the last section liquidus, solidus, and some subsolidus relations in the system were determined by means of the DTA. Several quenching runs were done to make sure some melting relations and the results are listed in Table 9. Copper-bismuth sulfide melt cannot be quenched to "glass" as widely known in the common metallic system. Then, the evidence of melting was based on a change in the appearance of the material

Table 9. Results of experimental runs for melting relations.

Cu <sub>2</sub> S mol%	Temp. °C	Time, hours	Products
20.0	600	76	CuBi <sub>3</sub> S <sub>5</sub> + Bi <sub>2</sub> S <sub>3</sub>
	625	48	CuBi <sub>3</sub> S <sub>5</sub> + Bi <sub>2</sub> S <sub>3</sub>
	650	48	Bi <sub>2</sub> S <sub>3</sub> + L
25.0	635	48	CuBi <sub>3</sub> S <sub>5</sub>
	650	48	Bi <sub>2</sub> S <sub>3</sub> + L
37.5	550	120	Cu <sub>3</sub> Bi <sub>5</sub> S <sub>9</sub> ss
	630	216	CuBi <sub>3</sub> S <sub>5</sub> + L
	675	72	L
40.0	550	120	Cu <sub>3</sub> Bi <sub>5</sub> S <sub>9</sub> ss
	600	72	Cu <sub>3</sub> Bi <sub>5</sub> S <sub>9</sub> ss + L
50.0	520	120	Cu <sub>3</sub> BiS <sub>3</sub> ss + Cu <sub>3</sub> Bi <sub>5</sub> S <sub>9</sub> ss
	550	120	Cu <sub>3</sub> Bi <sub>5</sub> S <sub>9</sub> ss + L
	625	120	L
60.0	515	120	Cu <sub>3</sub> BiS <sub>3</sub> ss + Cu <sub>3</sub> Bi <sub>5</sub> S <sub>9</sub> ss
	530	96	Cu <sub>3</sub> Bi <sub>5</sub> S <sub>9</sub> ss + L
	550	96	Cu <sub>3</sub> Bi <sub>5</sub> S <sub>9</sub> ss + L
	556	120	L
75.0	500	120	Cu <sub>3</sub> BiS <sub>3</sub> ss (+ Cu <sub>9</sub> BiS <sub>6</sub> ss)
	535	2	Cu <sub>9</sub> BiS <sub>6</sub> ss + L
	580	2	L
80.0	575	2	Cu <sub>9</sub> BiS <sub>6</sub> ss + L

from a porous and coarse mass or aggregate of powder to a smooth, rounded, non-porous globules. Partial melting such as eutectic or peritectic, common in this system, in which the crystalline phase is in equilibrium with the melt at the run temperature, is not easily determined. It can be only deduced from grain size and textural relations in the quenched sample under microscopic observation. The stable crystalline phase at the run temperature is characteristically coarser grained and surrounded by the finer grained material representing the crystallized liquid.

Experiments on the bulk compositions of 20.0 mol% and 25.0 mol% Cu<sub>2</sub>S show the incongruent melting of CuBi<sub>3</sub>S<sub>5</sub> occur between 635°C and 650°C which is consistent with 649°C given by the DTA, and Cu<sub>3</sub>Bi<sub>5</sub>S<sub>9</sub> melts incongruently at 620°C ± 5°C. Solidus of eutectic melting between Cu<sub>3</sub>BiS<sub>3</sub> ss and Cu<sub>3</sub>Bi<sub>5</sub>S<sub>9</sub> ss should be between 520°C and 530°C from the result of quenching runs on the composition of 50.0 mol% and 60.0 mol% Cu<sub>2</sub>S, and at the temperature of 556°C just above 553°C given from the DTA for the liquidus of 60.0 mol% Cu<sub>2</sub>S composition only liquid phase could be observed. From the results of the quenching and the DTA experiments eutectic point between Cu<sub>3</sub>BiS<sub>3</sub> ss and Cu<sub>3</sub>Bi<sub>5</sub>S<sub>9</sub> ss is at 523 ± 5°C and about 65 mol% Cu<sub>2</sub>S in composition. As shown



in Table 9, the quenching experiments support the results from the DTA investigation.

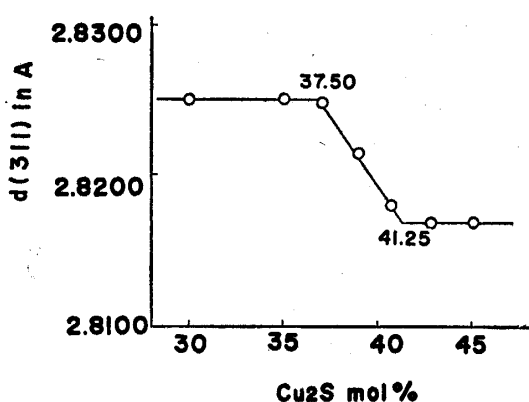
*Stability of  $\text{Cu}_3\text{Bi}_5\text{S}_9$  Solid Solution:* The phase,  $\text{Cu}_3\text{Bi}_5\text{S}_9$ , has been recognized by Nuffield<sup>7)</sup> (1947) during his study on cuprobismuth sulfosalts minerals. The phase has a fairly wide solid solution range at the higher temperature but is not stable at room temperature. Table 10 shows the results of several experiments in order to examine thermal and compositional stability of  $\text{Cu}_3\text{Bi}_5\text{S}_9$ . The phase is stable only above  $442^\circ \pm 3^\circ\text{C}$  to  $620^\circ \pm 5^\circ\text{C}$  which is incongruent melting temperature of  $\text{Cu}_3\text{Bi}_5\text{S}_9$ . Below  $442^\circ\text{C}$   $\text{Cu}_{24}\text{Bi}_{26}\text{S}_{51}$  and  $\text{CuBi}_3\text{S}_5$  are stable instead of  $\text{Cu}_3\text{Bi}_5\text{S}_9$  in this composition, but the breakdown reaction on cooling is sluggish. The extents of the solid solution field of  $\text{Cu}_3\text{Bi}_5\text{S}_9$  were determined by constructing curves of d-value versus composition. The d(311) reflection of  $\text{Cu}_3\text{Bi}_5\text{S}_9$  which synthesized at in various compositions at  $500^\circ\text{C}$  was measured precisely by the X-ray diffractometer with  $1/4^\circ$  per minute of goniometer rotation rate. An appropriate amount of silicon (99.9999% in purity) was mixed with sample and use as an internal standard. Results of measurement are listed in Table 11 and shown in Fig. 5. As clearly shown in Fig. 5, the solid solution area of  $\text{Cu}_3\text{Bi}_5\text{S}_9$  extends from 37.5 mol% to 41.25 mol%  $\text{Cu}_2\text{S}$  at  $500^\circ\text{C}$ . Maximum composition in  $\text{Cu}_2\text{S}$  mol% of the solid solution is 43.05 mol%  $\text{Cu}_2\text{S}$  at  $523^\circ \pm 5^\circ\text{C}$  that is the temperature of eutectic melting between  $\text{Cu}_3\text{Bi}_5\text{S}_9$  and  $\text{Cu}_3\text{Bi}_5\text{S}_9$ .

Table 10. Results of experimental runs for the stability of  $\text{Cu}_3\text{Bi}_5\text{S}_9$  solid solution.

$\text{Cu}_2\text{S}$ mol%	Temp. $^\circ\text{C}$	Time, hours	Products
35.00	500	120	$\text{Cu}_3\text{Bi}_5\text{S}_9$ ss + $\text{CuBi}_3\text{S}_5$
37.00	500	120	$\text{Cu}_3\text{Bi}_5\text{S}_9$ ss + $\text{CuBi}_3\text{S}_5$
37.50	400	182	$\text{Cu}_{24}\text{Bi}_{26}\text{S}_{51}$ + $\text{CuBi}_3\text{S}_5$
	500	120	$\text{Cu}_3\text{Bi}_5\text{S}_9$ ss
	600	78	$\text{Cu}_3\text{Bi}_5\text{S}_9$ ss
	625	216	$\text{CuBi}_3\text{S}_5$ + L
	500	120	$\text{Cu}_3\text{Bi}_5\text{S}_9$ ss
39.10	500	120	$\text{Cu}_3\text{Bi}_5\text{S}_9$ ss
40.00	430	168	$\text{Cu}_{24}\text{Bi}_{26}\text{S}_{51}$ + $\text{CuBi}_3\text{S}_5$
	440	168	$\text{Cu}_{24}\text{Bi}_{26}\text{S}_{51}$ + $\text{CuBi}_3\text{S}_5$
	445	144	$\text{Cu}_{24}\text{Bi}_{26}\text{S}_{51}$ + $\text{Cu}_3\text{Bi}_5\text{S}_9$ ss
	450	144	$\text{Cu}_{24}\text{Bi}_{26}\text{S}_{51}$ + $\text{Cu}_3\text{Bi}_5\text{S}_9$ ss
	500	120	$\text{Cu}_3\text{Bi}_5\text{S}_9$ ss
	550	120	$\text{Cu}_3\text{Bi}_5\text{S}_9$ ss
	600	78	$\text{Cu}_3\text{Bi}_5\text{S}_9$ ss + L
40.70	500	120	$\text{Cu}_3\text{Bi}_5\text{S}_9$ ss
42.86	500	120	$\text{Cu}_3\text{Bi}_5\text{S}_9$ ss (+ $\text{Cu}_3\text{Bi}_3\text{S}_3$ ss)
	550	120	$\text{Cu}_3\text{Bi}_5\text{S}_9$ ss + L
45.00	500	120	$\text{Cu}_3\text{Bi}_5\text{S}_9$ ss + $\text{Cu}_3\text{Bi}_3\text{S}_3$ ss

Table 11. Results of measurement on  $\text{Cu}_3\text{Bi}_5\text{S}_9$  ss d (311) spacing.

Comp. $\text{Cu}_2\text{S}$ mol%	Temp. (°C)	d (311) (Å)	Phase present
30.00	500	2.8250	$\text{Cu}_3\text{Bi}_5\text{S}_9$ ss + $\text{CuBi}_3\text{S}_5$
35.00	500	2.8253	$\text{Cu}_3\text{Bi}_5\text{S}_9$ ss + $\text{CuBi}_3\text{S}_5$
37.50	500	2.8248	$\text{Cu}_3\text{Bi}_5\text{S}_9$ ss
39.10	500	2.8214	$\text{Cu}_3\text{Bi}_5\text{S}_9$ ss
40.70	500	2.8179	$\text{Cu}_3\text{Bi}_5\text{S}_9$ ss
42.86	500	2.8169	$\text{Cu}_3\text{Bi}_5\text{S}_9$ ss + $\text{Cu}_3\text{Bi}_3\text{S}_3$ ss
45.00	500	2.8170	$\text{Cu}_3\text{Bi}_5\text{S}_9$ ss + $\text{Cu}_3\text{Bi}_3\text{S}_3$ ss

Fig. 5. Determination for the solid solution limit of  $\text{Cu}_3\text{Bi}_5\text{S}_9$  ss. Relations of d-value versus  $\text{Cu}_2\text{S}$  mol% at 500°C

*Phase Relations of Cuprobismutite and Emplectite:* Table 12 shows results of some experiments to examine the phase relations of cuprobismutite and emplectite. All experiments on the mixture of  $\text{Cu}_2\text{S}$  and  $\text{Bi}_2\text{S}_3$  in the ratio of 1:1 which corresponds to emplectite in natural occurrence produced always cuprobismutite

Table 12. Results of experimental runs for cuprobismutite and emplectite.

Composition $\text{Cu}_2\text{S}$ mol%	Starting materials	Temp. (°C)	Time (days)	Products
50.0	$\text{Cu}_2\text{S} + \text{Bi}_2\text{S}_3$	480	7	wt + $\text{Cu}_3\text{Bi}_5\text{S}_9$
50.0	$\text{Cu}_2\text{S} + \text{Bi}_2\text{S}_3$	460	7	cpb (+wt)
50.0	$\text{Cu}_2\text{S} + \text{Bi}_2\text{S}_3$	400	14	cpb (+wt)
*50.0	$\text{Cu}_3\text{Bi}_3\text{S}_3 + \text{Cu}_3\text{Bi}_5\text{S}_9$	250	14	emp (+wt)
49.0	$\text{Cu}_2\text{S} + \text{Bi}_2\text{S}_3$	400	21	cpb (+wt)
48.0	$\text{Cu}_2\text{S} + \text{Bi}_2\text{S}_3$	400	21	cpb
48.0	$\text{Cu}_3\text{Bi}_3\text{S}_3 + \text{Cu}_3\text{Bi}_5\text{S}_9$	400	14	cpb
47.0	$\text{Cu}_2\text{S} + \text{Bi}_2\text{S}_3$	400	26	cpb (+ $\text{Cu}_3\text{Bi}_5\text{S}_9$ )

\* Starting materials pressed by the oil press at 1 ton/cm<sup>2</sup> to make compressed cylindrical block before heating.

wt: wittichenite

cpb: cuprobismutite

emp: emplectite

taking with a small quantity of wittichenite ( $\text{Cu}_3\text{BiS}_3$ ) above  $400^\circ\text{C}$ , and emplectite never appeared as a stable phase at high temperature. From the results of the experiment shown in Table 12 the composition of cuprobismutite seems to be 48 mol%  $\text{Cu}_2\text{S}$ , and then chemical formula of this phase should be written as  $\text{Cu}_{24}\text{Bi}_{26}\text{S}_{51}$ . Cuprobismutite decomposes at  $473^\circ \pm 5^\circ\text{C}$  as determined by means of the DTA before, and quenching results does not contradict it.

Table 13. The data of X-ray diffraction for synthetic emplectite

(1)		(2)		
d	I	d	I	hkl
7.31	45	7.255	36	002
5.64	11	5.644	4	101
5.04	7	5.028	3	
4.70	34	4.681	29	102
4.55	9			
3.97	9	3.962	5	
3.83	6			
3.63	12	3.625	10	004
3.57	26			
3.53	12			
3.23	100	3.216	100	111
3.13	86	3.119	77	104
3.07	78	3.064	60	200
3.05	79	3.046	83	013
3.01	15			
2.95	7	3.000	16	201
2.858	18			
2.831	20	2.823	18	202
2.730	7	2.721	7	113
2.644	9			
2.600	7	2.588	7	203
2.522	8	2.515	4	
2.417	5	2.417	8	006
2.335	46	2.331	48	204
2.298	9	2.290	8	212
2.254	18	2.248	17	106
2.166	39	2.160	42	213
1.961	18	2.027	5	301
1.895	7	1.899	6	206
1.859	23	1.856	29	215

(1) Synthetic emplectite

(2) Natural emplectite by Buhlmann<sup>26)</sup>

(Tannenbaum, Saxony)

Only one experiment was successful to synthesize emplectite as also shown in Table 12.  $\text{Cu}_3\text{BiS}_3$  and  $\text{Cu}_3\text{Bi}_5\text{S}_9$  were weighed exactly to make a bulk composition to 50 mol%  $\text{Cu}_2\text{S}$ , mixed thoroughly, and then made a cylindrical compressed piece,  $5\text{ mm}\phi \times 6\text{ mm}$  in size, by the simple squeeze type oil press at one ton/cm<sup>2</sup> of pressure. The piece sealed into an evacuated glass tube and heated at 250°C for 26 days. X-ray powder pattern of product, shown in Table 13, is in good agreement with one of natural emplectite described by Buhlmann<sup>26)</sup>. The DTA curve of synthesized emplectite shows a weak endothermic peak beginning at about 360°C before melting. It is quite easy to conclude that this peak represents the transformation from emplectite to cuprobismutite if they are surely in dimorphous relation as mentioned by Nuffield<sup>12)</sup> and Buhlmann<sup>15)</sup>, but any positive evidence to interpret this peak has not been obtained yet. Active investigations by means of high temperature X-ray diffraction are being continued now to elucidate the relationship between both phases. Anyway, emplectite supposed to be certainly stable up to 360°C, while cuprobismutite which is synthesized at higher temperature and then kept in vacuum almost 5 years at room temperature has not changed at all. There are still many problems which must be solved as for the relationship between emplectite and cuprobismutite.

*Examination of Klaprothite and Dognacskite:* In order to ascertain the reliability of the existence of klaprothite and dognacskite, several quenching runs were practised and the results are shown in Table 14. No compound with the composition of  $3\text{Cu}_2\text{S} \cdot 2\text{Bi}_2\text{S}_3$  and  $\text{Cu}_2\text{S} \cdot 2\text{Bi}_2\text{S}_3$ , corresponding to the composition reported for klaprothite and dognacskite respectively, was synthesized at any temperature, and quenching products were always mixtures of two phases. From consideration of the results, it seems most reasonable to conclude that klaprothite and dognacskite are untrustworthy species as minerals.

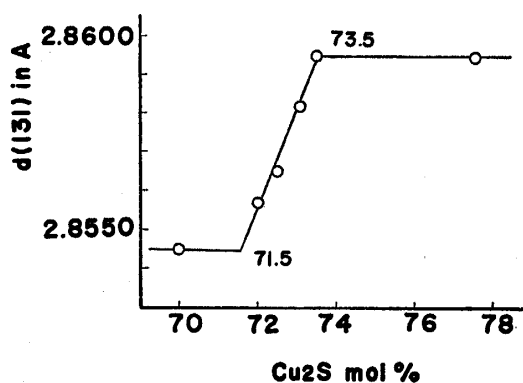
Table 14. Results of experimental runs for klaprothite and dognacskite.

Composition Cu <sub>2</sub> S mol%	Starting materials	Temp. (°C)	Time (days)	Products
32.0	$\text{Cu}_2\text{S} + \text{Bi}_2\text{S}_3$	500	5	$\text{Cu}_3\text{Bi}_5\text{S}_9$ ss + $\text{CuBi}_3\text{S}_5$
33.0	$\text{Cu}_2\text{S} + \text{Bi}_2\text{S}_3$	500	5	$\text{Cu}_3\text{Bi}_5\text{S}_9$ ss + $\text{CuBi}_3\text{S}_5$
33.3	$\text{Cu}_2\text{S} + \text{Bi}_2\text{S}_3$	500	5	$\text{Cu}_3\text{Bi}_5\text{S}_9$ ss + $\text{CuBi}_3\text{S}_5$
33.3	$\text{Cu}_3\text{BiS}_3$ ss + $\text{CuBi}_3\text{S}_5$	400	14	$\text{Cu}_3\text{Bi}_5\text{S}_9$ ss + $\text{Cu}_{24}\text{Bi}_{26}\text{S}_{51}$
33.3	$\text{Cu}_3\text{BiS}_3$ ss + $\text{CuBi}_3\text{S}_5$	300	32	$\text{Cu}_3\text{Bi}_5\text{S}_9$ ss + $\text{Cu}_{24}\text{Bi}_{26}\text{S}_{51}$
60.0	$\text{Cu}_2\text{S} + \text{Bi}_2\text{S}_3$	500	5	$\text{Cu}_3\text{BiS}_3$ ss + $\text{Cu}_3\text{Bi}_5\text{S}_9$ ss
60.0	$\text{Cu}_3\text{BiS}_3 + \text{Cu}_{24}\text{Bi}_{26}\text{S}_{51}$	500	5	$\text{Cu}_3\text{BiS}_3$ ss + $\text{Cu}_3\text{Bi}_5\text{S}_9$ ss
60.0	$\text{Cu}_2\text{S} + \text{Bi}_2\text{S}_3$	400	14	$\text{Cu}_3\text{BiS}_3$ ss + $\text{Cu}_{24}\text{Bi}_{26}\text{S}_{51}$
60.0	$\text{Cu}_3\text{BiS}_3 + \text{Cu}_{24}\text{Bi}_{26}\text{S}_{51}$	300	32	$\text{Cu}_3\text{BiS}_3$ ss + $\text{Cu}_{24}\text{Bi}_{26}\text{S}_{51}$
60.0	$\text{Cu}_3\text{BiS}_3 + \text{Cu}_{24}\text{Bi}_{26}\text{S}_{51}$	200	88	$\text{Cu}_3\text{BiS}_3$ ss + $\text{Cu}_{24}\text{Bi}_{26}\text{S}_{51}$

*Stability of  $\text{Cu}_3\text{BiS}_3$  Solid Solution:* Synthetic  $\text{Cu}_3\text{BiS}_3$  is identical with natural wittichenite in every respect as shown in the case of X-ray powder pattern of Table 4. Though the phase has the composition of  $\text{Cu}_3\text{BiS}_3$  at room temperature, compositional stability range of  $\text{Cu}_3\text{BiS}_3$  shifts towards  $\text{Cu}_2\text{S}$  poor composition at higher temperature. Extent of the solid solution field of  $\text{Cu}_3\text{BiS}_3$  were determine by X-ray method. The  $d(131)$  spacing of  $\text{Cu}_3\text{BiS}_3$  solid solution synthesized at  $500^\circ\text{C}$  in several different compositions were carefully measured and plotted versus composition as shown in Table 15 and Fig. 6. From the  $d$  versus composition curve, solid solution of  $\text{Cu}_3\text{BiS}_3$  extends from 73.5 mol% to 71.5 mol%  $\text{Cu}_2\text{S}$  at  $500^\circ\text{C}$ .  $\text{Cu}_3\text{BiS}_3$  ss melts incongruently at  $527^\circ \pm 5^\circ\text{C}$  at nearly 72.5 mol%  $\text{Cu}_2\text{S}$ .

Table 15. Results of measurement of  $d(131)$  spacing on  $\text{Cu}_3\text{BiS}_3$  ss.

Composition $\text{Cu}_2\text{S}$ mol%	Temp. ( $^\circ\text{C}$ )	$d(131)$ ( $\text{A}$ )	Phase present
70.0	500	2.8545	$\text{Cu}_3\text{BiS}_3$ ss + $\text{Cu}_9\text{BiS}_6$
72.0	500	2.8557	$\text{Cu}_3\text{BiS}_3$ ss
72.5	500	2.8565	$\text{Cu}_3\text{BiS}_3$ ss
73.0	500	2.8583	$\text{Cu}_3\text{BiS}_3$ ss
73.5	500	2.8595	$\text{Cu}_3\text{BiS}_3$ ss
77.5	500	2.8595	$\text{Cu}_3\text{BiS}_3$ ss + $\text{Cu}_3\text{Bi}_5\text{S}_9$ ss

Fig. 6. Determination for the solid solution limit of  $\text{Cu}_3\text{BiS}_3$ . Relations of  $d$ -value versus  $\text{Cu}_2\text{S}$  mol% at  $500^\circ\text{C}$ .

#### High Temperature X-ray Study for $\text{Cu}_2\text{S}$ Rich Portion:

Among the  $\text{Cu}_2\text{S}-\text{Bi}_2\text{S}_3$  system the portion near  $\text{Cu}_2\text{S}$  is the most difficult to make clear the phase relations, because of difficulty of quenching to keep the phases at run temperature, and less reproducibility of X-ray powder pattern. In this paper  $\text{Cu}_9\text{BiS}_6$  phase (which has fairly wide solid solution field at high temperature) is supposed to be an independent phase from  $\text{Cu}_2\text{S}$  solid solution, but both of them are supposed to have a very similar structure at the high temperature, then it is still difficult to identify both phases from each other.

Some high temperature X-ray investigation was practiced. Fig. 7 shows

high temperature X-ray diffraction pattern of two high temperature modifications of chalcocite I (cubic) and II (hexagonal) and  $\text{Cu}_9\text{BiS}_6$  phase. As shown in the figure, two reflections between  $25^\circ$  and  $30^\circ$  in  $2\theta$  of  $\text{Cu}_9\text{BiS}_6$  seem to correspond to (111) and (200) reflection of cubic phase of chalcocite and other two between  $45^\circ$  and  $50^\circ$  in  $2\theta$ , to (110) and (103) reflections of hexagonal phase of chalcocite. Quenched products from the temperature above  $400^\circ\text{C}$  usually

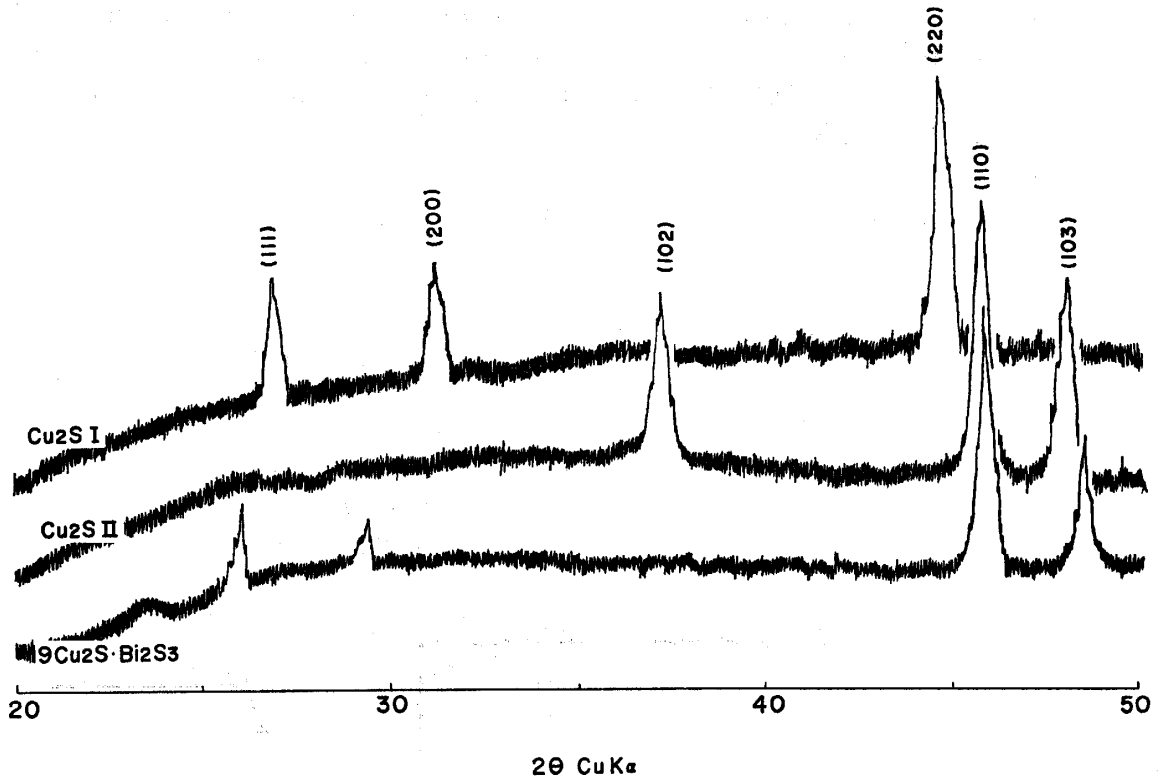


Fig. 7. High temperature X-ray diffraction patterns of  $\text{Cu}_9\text{BiS}_6$  and chalcocite

Table 16. Results of high temperature X-ray study on  $\text{Cu}_9\text{BiS}_6$  solid solution.

Composition $\text{Cu}_2\text{S}$ mol%	room temp.**	298°C	350°C	400°C	480°C
100.0	CcIII	CcII			CcI
97.5	CcIII + $\text{Cu}_9\text{BiS}_6^*$			CcII	CcI
95.0	$\text{Cu}_9\text{BiS}_6^*$	CcII + wt	CcII ? + wt		
90.0	$\text{Cu}_9\text{BiS}_6^*$	CcII + wt		$\text{Cu}_9\text{BiS}_6$ (+wt)	$\text{Cu}_9\text{BiS}_6$
85.0	$\text{Cu}_9\text{BiS}_6^*$			$\text{Cu}_9\text{BiS}_6$ + wt	$\text{Cu}_9\text{BiS}_6$

CcIII : chalcocite orthorhombic low form

CcII : chalcocite hexagonal high temp. form

CcI : chalcocite cubic high temp. form

$\text{Cu}_9\text{BiS}_6^*$  : quenched pattern of  $\text{Cu}_9\text{BiS}_6$

wt : wittichenite

\*\* : X-ray diffraction was taken at room temperature on the quenched sample from  $500^\circ\text{C}$ .

indicates several weak additional reflections. Results of high temperature X-ray studies are listed in Table 16. Experiments on the composition containing 97.5 mol%  $\text{Cu}_2\text{S}$  give only X-ray patterns of chalcocite, hexagonal pattern at  $390^\circ\text{C}$  and cubic pattern at  $480^\circ\text{C}$ . Then considering the evidence chalcocite solid solution dissolves  $\text{Bi}_2\text{S}_3$  molecule at least 2.5 mol%. Small quantity of wittichenite coexists with chalcocite II below  $350^\circ\text{C}$  at the composition of 95.0 mol%  $\text{Cu}_2\text{S}$ . In experiments on the composition of 90.0 mol%  $\text{Cu}_2\text{S}$  chalcocite II and wittichenite assemblage at lower temperature change into  $\text{Cu}_9\text{BiS}_6$  and wittichenite assemblage at  $400^\circ\text{C}$ , and the homogeneous  $\text{Cu}_9\text{BiS}_6$  at  $480^\circ\text{C}$  with ascending temperature. On the basis of these data, it seems reasonable to assume that  $\text{Cu}_9\text{BiS}_6$  is independent phase from chalcocite and stable only above the temperature between  $350^\circ\text{C}$  and  $400^\circ\text{C}$ .  $\text{Cu}_9\text{BiS}_6$  melt incongruently at nearly  $650^\circ\pm 10^\circ\text{C}$ . From results of high temperature X-ray investigations, quenching runs, and DTA experiments, solid solution field of  $\text{Cu}_9\text{BiS}_6$  extends to 87 mol%  $\text{Cu}_2\text{S}$  at  $450^\circ\text{C}$ , 82 mol%  $\text{Cu}_2\text{S}$  at  $500^\circ\text{C}$  and about 78 mol%  $\text{Cu}_2\text{S}$  in maximum at  $526^\circ\text{C}$ .

### Summary and Discussions

The summarized phase diagram of the  $\text{Cu}_2\text{S}-\text{Bi}_2\text{S}_3$  system is shown in Fig. 8, and the temperatures of the phase changing reactions are listed in Table 17.

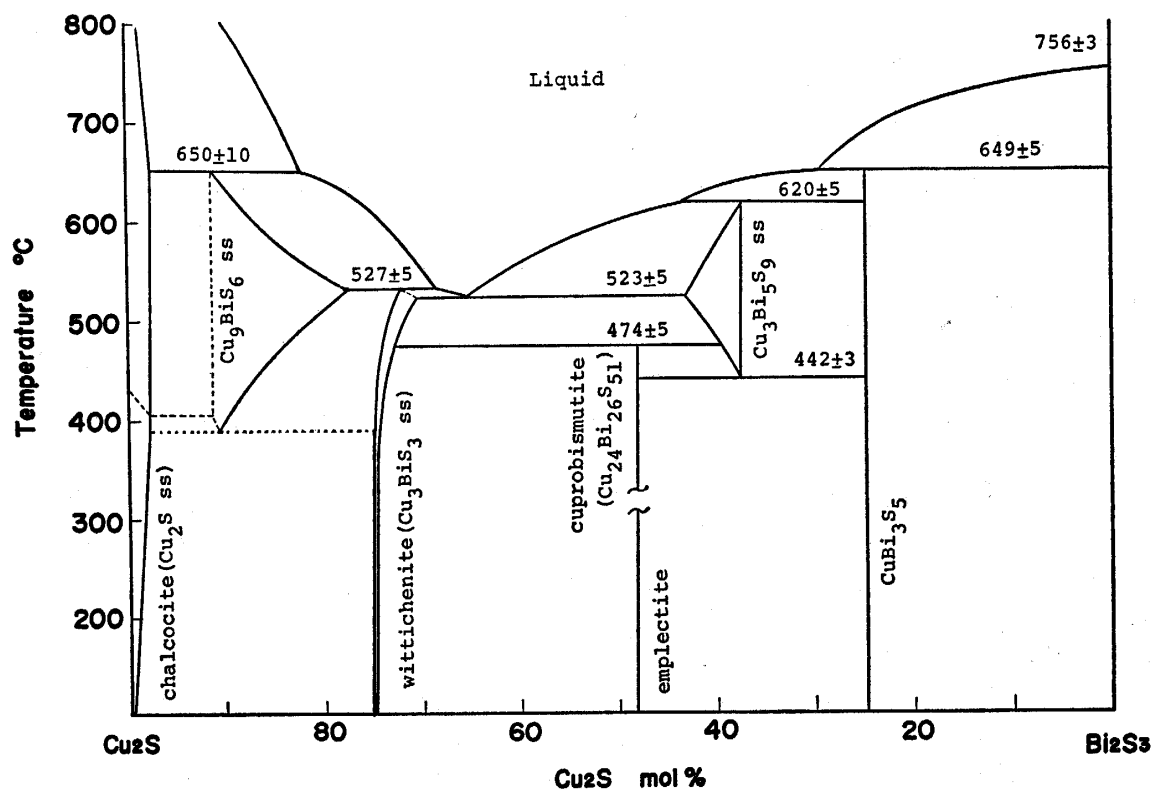


Fig. 8. Phase diagram of the  $\text{Cu}_2\text{S}-\text{Bi}_2\text{S}_3$  system

Table 17. List of the reaction temperature in the  $\text{Cu}_2\text{S}$ - $\text{Bi}_2\text{S}_3$  system.

Congruent melting of $\text{Bi}_2\text{S}_3$	$756^\circ \pm 3^\circ\text{C}$
Incongruent melting of $\text{CuBi}_3\text{S}_5$	$649^\circ \pm 5^\circ\text{C}$
Incongruent melting of $\text{Cu}_3\text{Bi}_5\text{S}_9$	$620^\circ \pm 5^\circ\text{C}$
Lower stability limit of $\text{Cu}_3\text{Bi}_5\text{S}_9$	$442^\circ \pm 5^\circ\text{C}$
Decomposition of $\text{Cu}_{24}\text{Bi}_{26}\text{S}_{51}$	$474^\circ \pm 5^\circ\text{C}$
Incongruent melting of $\text{Cu}_3\text{BiS}_3$	$527^\circ \pm 5^\circ\text{C}$
Eutectic of $\text{Cu}_3\text{BiS}_3$ - $\text{Cu}_3\text{Bi}_5\text{S}_9$	$523^\circ \pm 5^\circ\text{C}$
Incongruent melting of $\text{Cu}_9\text{BiS}_6$	$650^\circ \pm 10^\circ\text{C}$
Lower stability limit of $\text{Cu}_9\text{BiS}_6$	$350^\circ - 400^\circ\text{C}$

Crystalline phases in the system are  $\text{Cu}_2\text{S}$ (chalcocite),  $\text{Cu}_9\text{BiS}_6$ ,  $\text{Cu}_3\text{BiS}_3$  (wittichenite),  $\text{Cu}_{24}\text{Bi}_{26}\text{S}_{51}$  (cuprobismutite),  $\text{CuBiS}_2$  or  $\text{Cu}_{24}\text{Bi}_{26}\text{S}_{51}$  (emlectite),  $\text{Cu}_3\text{Bi}_5\text{S}_9$ ,  $\text{CuBi}_3\text{S}_5$ , and  $\text{Bi}_2\text{S}_3$  (bismuthinite). Among them  $\text{Cu}_9\text{BiS}_6$ ,  $\text{Cu}_3\text{Bi}_5\text{S}_9$ , and  $\text{CuBi}_3\text{S}_5$  have not been found in nature, and the former two phases,  $\text{Cu}_9\text{BiS}_6$  and  $\text{Cu}_3\text{Bi}_5\text{S}_9$ , could not be expected to be found in nature hereafter because of their unstability at low temperature as shown in Fig. 8, while  $\text{CuBi}_3\text{S}_5$  phase has a possibility in future.  $\text{CuBi}_3\text{S}_5$  is stable below  $649^\circ \pm 5^\circ\text{C}$  and the phase melts in congruently at this temperature to  $\text{Bi}_2\text{S}_3$  and liquid.

$\text{Cu}_3\text{Bi}_5\text{S}_9$  is stable in temperature range between  $442^\circ \pm 5^\circ\text{C}$  and  $620^\circ \pm 5^\circ\text{C}$  which is incongruent melting point of this phase. Buhlmann<sup>15)</sup> gives  $688^\circ \pm 5^\circ\text{C}$  in his phase diagram to the temperature of incongruent melting of  $\text{Cu}_3\text{Bi}_5\text{S}_9$ . His diagram shows a little lower temperature than our results in general, but the difference of both data does not exceed 10 degrees and within allowance of the measurements. Incongruent melting temperature of  $\text{Cu}_3\text{Bi}_5\text{S}_9$  is only the big discrepancy between both results.  $\text{Cu}_3\text{Bi}_5\text{S}_9$  dissolves a considerable amount of  $\text{Cu}_2\text{S}$  molecule, and solid solution limit is the composition of 43.5 mol%  $\text{Cu}_2\text{S}$  in maximum at  $523^\circ\text{C}$ . Phase relations of cuprobismuthite and emlectite still have a problem which has to be elucidated. Cuprobismutite that was once reported as  $4\text{Cu}_2\text{S} \cdot 3\text{Bi}_2\text{S}_3$  by Hillebrand<sup>9)</sup> has a composition of 48 mol%  $\text{Cu}_2\text{S}$  and 52 mol%  $\text{Bi}_2\text{S}_3$  and decomposes at  $473^\circ \pm 5^\circ\text{C}$  into  $\text{Cu}_3\text{BiS}_3$  and  $\text{Cu}_3\text{Bi}_5\text{S}_9$ . Lower stability limit of cuprobismutite has not been determined but after 5 years kept in vacuum at room temperature cuprobismutite has not changed at all. X-ray powder pattern of synthesized phase is shown in Table 6 with those of natural cuprobismutite by Berry and Thompson<sup>27)</sup>. On the other hand emlectite, of which accurate composition is not determined yet, was synthesized at  $250^\circ\text{C}$  for 26 days from a compressed cylindrical block sample, mixture of  $\text{Cu}_3\text{BiS}_3$  and  $\text{Cu}_3\text{Bi}_5\text{S}_9$ , 50 mol%  $\text{Cu}_2\text{S}$  in bulk composition. The DTA curve of synthesized emlectite shows weak endothermic thermal effect beginning at about  $360^\circ\text{C}$ , and before it no effect is seen. It seems to be sure emlectite is stable below about  $360^\circ\text{C}$ , but is not sure to transform into cuprobismutite above this temperature as suggested by Nuffield<sup>12)</sup> and Buhlmann<sup>15)</sup>.



Buhlmann suggested 290°C as transformation temperature from emplectite to cuprobismutite, then even if the endothermic effect at 360°C is supposed to represent the transition, 70 degrees difference is inconsistent. There is still high possibility that emplectite and cuprobismutite are in dimorphous relations, but conclusion will be laid until after more detailed investigation. Even though they are dimorphous, transformation from cuprobismutite to emplectite should be sluggish because it has never been succeeded to synthesize emplectite by means of annealing cuprobismutite formed at higher temperature.

Synthetic wittichenite, Cu<sub>3</sub>BiS<sub>3</sub>, has identical properties in every respects with natural wittichenite. X-ray powder diffraction data are shown in Table 4 comparing with those of natural wittichenite by Nuffield<sup>7)</sup>. At high temperature compositional stability range of Cu<sub>3</sub>BiS<sub>3</sub> solid solution shifts towards less Cu<sub>2</sub>S molecule, and this phase melts incongruently at 527° ± 5°C in 73.0 mol% Cu<sub>2</sub>S. The eutectic point between Cu<sub>3</sub>BiS<sub>3</sub> ss and Cu<sub>3</sub>Bi<sub>5</sub>S<sub>9</sub> ss is 527° ± 5°C at about 65 mole% Cu<sub>2</sub>S.

Klaprothite and dognacskite have not appeared in the study. Both minerals having Cu<sub>6</sub>Bi<sub>4</sub>S<sub>9</sub> and Cu<sub>2</sub>Bi<sub>4</sub>S<sub>7</sub> in composition could not be expected to be found in nature hereafter. However, about klaprothite Springer<sup>28)</sup> suggested quite recently some possibility of dimorphous relation with emplectite and of identical species with cuprobismutite.

Cu<sub>9</sub>BiS<sub>6</sub>, supposing to have the similar structure of high temperature forms of chalcocite, is stable below 650°C and above around 400°C, but lower stability limit has not been determined. Cu<sub>9</sub>BiS<sub>6</sub> dissolves considerable amount of Bi<sub>2</sub>S<sub>3</sub> molecule and solid solution field extends to 87 mol% Cu<sub>2</sub>S at 450°C, 78 mol% Cu<sub>2</sub>S in maximum at 527°C.

The properties of the crystalline phases, such as optical and crystallographic, will be described minutely in another paper.

## References

- 1) T. Petersen: *Ann. Phys. Chem.*, **134**, 64–106 (1868)
- 2) F. Sandberger: *Neues Jb. Min.*, **415**, 385–432 (1868)
- 3) J. Murdoch: "Microscopic determination of the opaque minerals" New York, (1916)
- 4) H. Schneiderhöhn and P. Ramdohr: "Lehrbuch der Erzmikroskopie" Bd. II, Berlin (1931) p. 399
- 5) M. N. Short: "Microscopic determination of the ore minerals" U.S.G.S. Bull. 914 (1931) p. 120
- 6) C. Frondel et al. ed.: "Dana's system of mineralogy" vol. 1, John Wiley & Sons N. Y. (1944) p. 418
- 7) E. W. Nuffield: *Econ. Geol.*, **42**, 147–160 (1947)
- 8) P. Ramdohr: "The ore minerals and their intergrowth" Pergamon Press N. Y. (1969) p. 711
- 9) W. F. Hillebrand: *Am. J. Sci.*, **27**, 355–357 (1884)
- 10) E. Dana: "Dana's system of mineralogy" John Wiley & Sons, N. Y. (1892) p. 110
- 11) C. Palache: *Am. Mineral.*, **25**, 611–613 (1940)

- 12) E. W. Nuffield: *Am. Mineral.*, **37**, 447-452 (1952)
- 13) A. M. Gaudin and G. Dicke: *Econ. Geol.*, **34**, 214-230 (1939)
- 14) A. Sugaki and H. Shima: *Mem. Fac. Eng. Yamaguchi Univ.*, **15**, 33-47, (1965)
- 15) E. Buhlmann: *Neues Jb. Min. Monat.*, Heft 4, 137-141 (1971)
- 16) A. Sugaki and H. Shima: *Mem. Fac. Eng. Yamaguchi Univ.*, **15**, 15-32 (1965)
- 17) G. Kullerud and H. S. Yorder: *Econ. Geol.*, **54**, 533-572 (1959)
- 18) A. Sugaki and H. Shima: *Mem. Fac. Eng. Yamaguchi Univ.*, **16**, 99-108, (1965) (in Japanese)
- 19) E. Jensen: *Am. J. Sci.*, **240**, 695-709 (1942)
- 20) F. C. Kracek: *Trans. Amer. Geophys. Union*, **27**, 364-374 (1946)
- 21) G. Kullerud and R. A. Yund: *Jour. Petrology*, **3**, 126-175 (1962)
- 22) J. A. Dunne and P. F. Kerr: *Am. Mineral.*, **46**, 1-12 (1961)
- 23) G. H. Moh: *Neues Jb. Min. Abh.*, **111**, 227-263 (1969)
- 24) M. V. Zakharov: *Chem. Abstr.*, **36**, 2200 (1939)
- 15) H. Shima: *Dr. Thesis of Tohoku Univ.* (1965)
- 26) E. Buhlmann: *PhD. Thesis of Heidelberg Univ.* (1965)
- 27) L. G. Berry and R. M. Thompson: "X-ray powder data for ore minerals" *Geol. Soc. Amer.*, N. Y. (1962) p. 143
- 28) G. Springer and S. Demirsoy: *Neues Jb. Min. Monat.*, Heft 1, 32-37, (1969)